

# Analysis on the temperature dependent structural properties of $\text{Li}_2\text{CO}_3$ doped $(\text{Ba,Sr})\text{TiO}_3$ ceramics

Yong-Su Ham · Seok Woo Yun · Jung-Hyuk Koh

Received: 17 November 2009 / Accepted: 20 October 2010 / Published online: 30 October 2010  
© Springer Science+Business Media, LLC 2010

**Abstract** We have fabricated various amount of  $\text{Li}_2\text{CO}_3$  doped  $(\text{Ba,Sr})\text{TiO}_3$  (BST) ceramics for LTCCs (Low Temperature Co-fired Ceramics) applications through the conventional sintering method. By introducing  $\text{Li}_2\text{CO}_3$  into BST ceramics, the sintering temperature was decreased from  $1350^\circ\text{C}$  to  $900^\circ\text{C}$ . In this study, we discussed the crystalline and structural properties of  $\text{Li}_2\text{CO}_3$  doped BST ceramics. By scanning X-ray diffraction analysis, we found that 1, 3, and 5 wt%  $\text{Li}_2\text{CO}_3$  doped  $(\text{Ba,Sr})\text{TiO}_3$  ceramics have perovskite structure without any pyrochlore phases. Frequency dependent dielectric properties were analyzed and discussed. Scanning Electron Microscopy (SEM) images depending on the sintering temperature and dopants were prepared and discussed. The crystalline and dielectric properties of  $\text{Li}_2\text{CO}_3$  doped  $(\text{Ba,Sr})\text{TiO}_3$  were discussed.

**Keywords** Ferroelectrics · Dielectric response · SEM · BST

## 1 Introduction

Ferroelectrics are very attractive materials for wide range of applications. For the high frequency applications, they are very promising materials due to their nonlinear behavior of dielectric permittivity in electric field. Especially,  $(\text{Ba,Sr})\text{TiO}_3$  (hereafter BST) materials for low temperature co-fired ceramics (LTCCs) technologies have been attracted

attention to the field of microelectronic component applications due to its high dielectric permittivity, tunability, low dielectric losses and small leakage current density [1, 2]. LTCCs technologies have a unique ability to integrate passive components such as resistors, capacitors and inductors into a monolithic package for System on Packaging (SOP) applications.

However, the pure BST and BST-base materials are commonly sintered at high temperature over the  $1350^\circ\text{C}$ , which is too high to be used for the silver electrodes. To co-fire the ceramic and electrodes, electrode materials have to bear up against this high thermal energy. To endure the high thermal energy, expensive and noble electrode materials such as palladium and platinum were required. However, platinum electrodes have relatively lower electrical conductance and much expensive than silver electrodes. If the sintering temperature of BST ceramic can be lowered under  $900^\circ\text{C}$ , silver electrode was able to be employed as the inner electrodes of LTCCs.

Many researches have been conducted to reduce sintering temperature of functional ceramics by adding dopants such as  $\text{B}_2\text{O}_3$  [3],  $\text{La}_2\text{O}_3$  [4],  $\text{LiCO}_3$  [5],  $\text{CuV}_2\text{O}_6$  [6], and  $\text{CuO}$  [7]. By adding dopants to the ferroelectric or dielectric materials, dielectric permittivity can be decreased, while loss tangent increased. Moreover, by adding glass frits to the functional ceramics, the sintering temperature can be lowered drastically, while their dielectric properties were degraded by a large margin [8]. According to our previous study, the sintering temperature was decreased from  $1350^\circ\text{C}$  to  $900^\circ\text{C}$  by doping the  $\text{Li}_2\text{CO}_3$  to the BST ceramics [9].

In this study, we investigated the microstructure and electrical properties of various amount  $\text{Li}_2\text{CO}_3$  doped BST ceramics sintered at  $900^\circ\text{C}$ .

Y.-S. Ham · S. W. Yun · J.-H. Koh (✉)  
Department of Electronic Materials Engineering, Kwangwoon University,  
Seoul, South Korea  
e-mail: jhkoh@kw.ac.kr

## 2 Experiments

To make the BST powders, BaCO<sub>3</sub>, SrCO<sub>3</sub> and TiO<sub>2</sub> powders with high purity of 99.9% were used as raw materials. The raw materials were weighed and calculated to fabricate (Ba<sub>0.5</sub>Sr<sub>0.5</sub>)TiO<sub>3</sub> composition. The powders were mixed by employing the wet-milling process for 24 h and dried at 120°C for 24 h. The impurities and organic components were burned out at 600°C for 1.5 h and then calcined at 1100°C for 2 h and then slowly cooled down to room temperature with the rate of 3°C/min. The calcined Li<sub>2</sub>CO<sub>3</sub> doped BST powders were granulated with 100 mesh sieve to uniform the powder size. The Li<sub>2</sub>CO<sub>3</sub> doped BST ceramic pellets were fabricated by employing the 12 Φ mold with pressure of 1 ton. The fabricated Li<sub>2</sub>CO<sub>3</sub> doped BST ceramic pellets were sintered at various temperature from 900°C to 1350°C for 2 h.

The crystalline structure of the Li<sub>2</sub>CO<sub>3</sub> doped BST ceramic were analyzed by X-ray diffraction pattern. X-ray diffraction 2θ scans were measured by employing the Rigaku X-ray diffractometer with Cu-Kα source. To investigate the frequency dependent dielectric permittivity and dielectric loss, HP 4284A precision LCR meter was employed. The dielectric permittivity and dielectric loss were measured from 1 kHz to 100 kHz. The electrical properties of Li<sub>2</sub>CO<sub>3</sub> doped BST ceramics were measured at room temperature by employing Keithly 6517A electrometer/high resistance meter. The electrical resistivity of various amount of Li<sub>2</sub>CO<sub>3</sub> doped BST ceramics was calculated in the linear section of electric field dependent leakage current density characteristics by considering its geometry. The microstructure of Li<sub>2</sub>CO<sub>3</sub> doped BST ceramics was investigated by employing the Field Emission Scanning Electron Microscopy (FE-SEM).

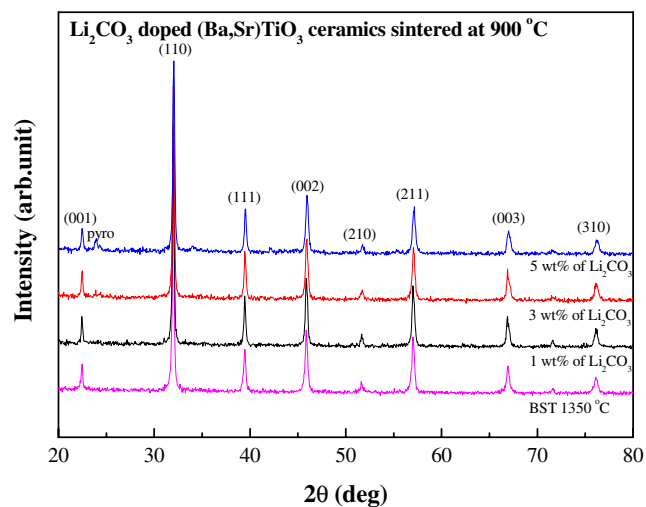


**Fig. 1** X-ray diffraction pattern of pure BST ceramic sintered at 1350°C and that of 1, 3 and 5 wt% Li<sub>2</sub>CO<sub>3</sub> doped BST ceramics sintered at 900°C

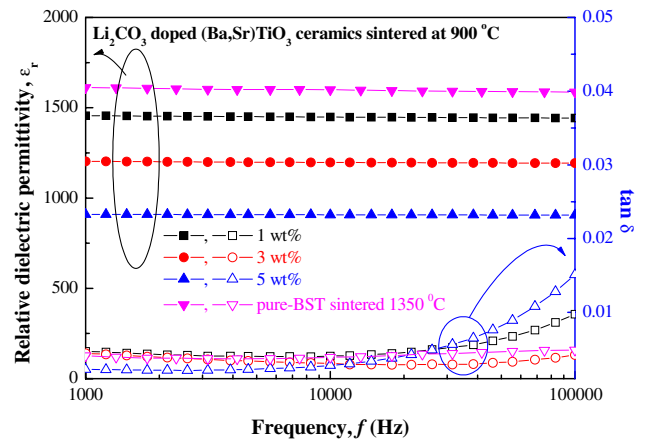


**Fig. 2** Frequency dependent relative dielectric permittivity and dielectric loss of 0, 1, 3 and 5 wt.% Li<sub>2</sub>CO<sub>3</sub> doped BST ceramics sintered at 1350°C and 900°C, which investigated from 1 to 100 kHz, respectively

## 3 Results and discussion

Figure 1 shows that the crystalline properties of 1, 3, and 5 wt.% Li<sub>2</sub>CO<sub>3</sub> doped BST ceramics sintered at 900°C and pure BST ceramic sintered at 1350°C. As shown in the Fig. 1, X-ray diffraction patterns of 1, 3, and 5 wt.% Li<sub>2</sub>CO<sub>3</sub> doped BST ceramics sintered at 900°C were similar to that of pure BST ceramic sintered at 1350°C. This result means that the Li<sub>2</sub>CO<sub>3</sub> doped BST ceramics were crystallized around 900°C. From the X-ray diffraction patterns, we did not find any pyrochlore phase in the Fig. 1 except for the 5 wt.% Li<sub>2</sub>CO<sub>3</sub> doped BST ceramic. We found that the pyrochlore phase of 5 wt.% Li<sub>2</sub>CO<sub>3</sub> doped BST ceramic is related with the over sintering. From the X-ray diffraction analysis, we found that Li<sub>2</sub>CO<sub>3</sub> doped BST ceramics have perovskite structure. The lattice parameters of BST were

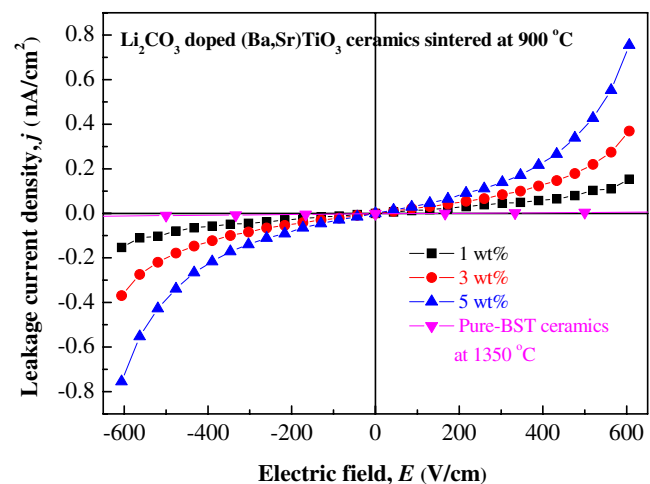


**Fig. 3** Leakage current density of 0, 1, 3 and 5 wt.% Li<sub>2</sub>CO<sub>3</sub> doped BST ceramics sintered at 1350°C and 900°C, respectively. The electric field was applied from -606 V/cm to +606 V/cm

calculated from the X-ray diffraction analysis. To calculate the lattice parameters of  $\text{Li}_2\text{CO}_3$  doped BST ceramics, *Nelson-Riley* extrapolation function with least mean square method was employed. The equation can be expressed as follows.

$$\frac{C_{\cos\theta} - C_0}{C_0} = A \cdot \cos^2\theta \left( \frac{1}{\sin\theta} + \frac{1}{\theta} \right) \quad (1)$$

where  $C_{\cos\theta}$  is an interplane distance calculated from the apparent Bragg peak position at  $2\theta$  and  $A$  is a fitting coefficient. From the calculated lattice parameter, the lattice parameters of  $\text{Li}_2\text{CO}_3$  doped BST ceramics were decreased with the increased amount of  $\text{Li}_2\text{CO}_3$  and they show the

pseudo-cubic states. The calculated lattice parameters of 1, 3 and 5 wt.% of  $\text{Li}_2\text{CO}_3$  doped BST ceramics were 3.955 Å, 3.951 Å and 3.947 Å, respectively. We found this decreased lattice parameter probably come from the strong chemical bonding energy and the increased density of BST ceramics. The electro negativity of Li, Ba, and Sr were 0.98, 0.89, and 0.95, respectively. The electro negativity of Li was bigger than Ba and Sr. We found that increased Li addition play a role to make more strong bonding with oxygen. In an ideal cubic perovskite  $\text{ABO}_3$ , the coordination number of the A-site and B-site are 12 and 6, respectively. The ionic radius of  $\text{Li}^+$ ,  $\text{Ti}^{4+}$ ,  $\text{Ba}^{2+}$ , and  $\text{Sr}^{2+}$  were 0.76, 0.68, 1.35, and 1.12 Å, respectively. It mean that  $\text{Li}^+$  could occupy the A site

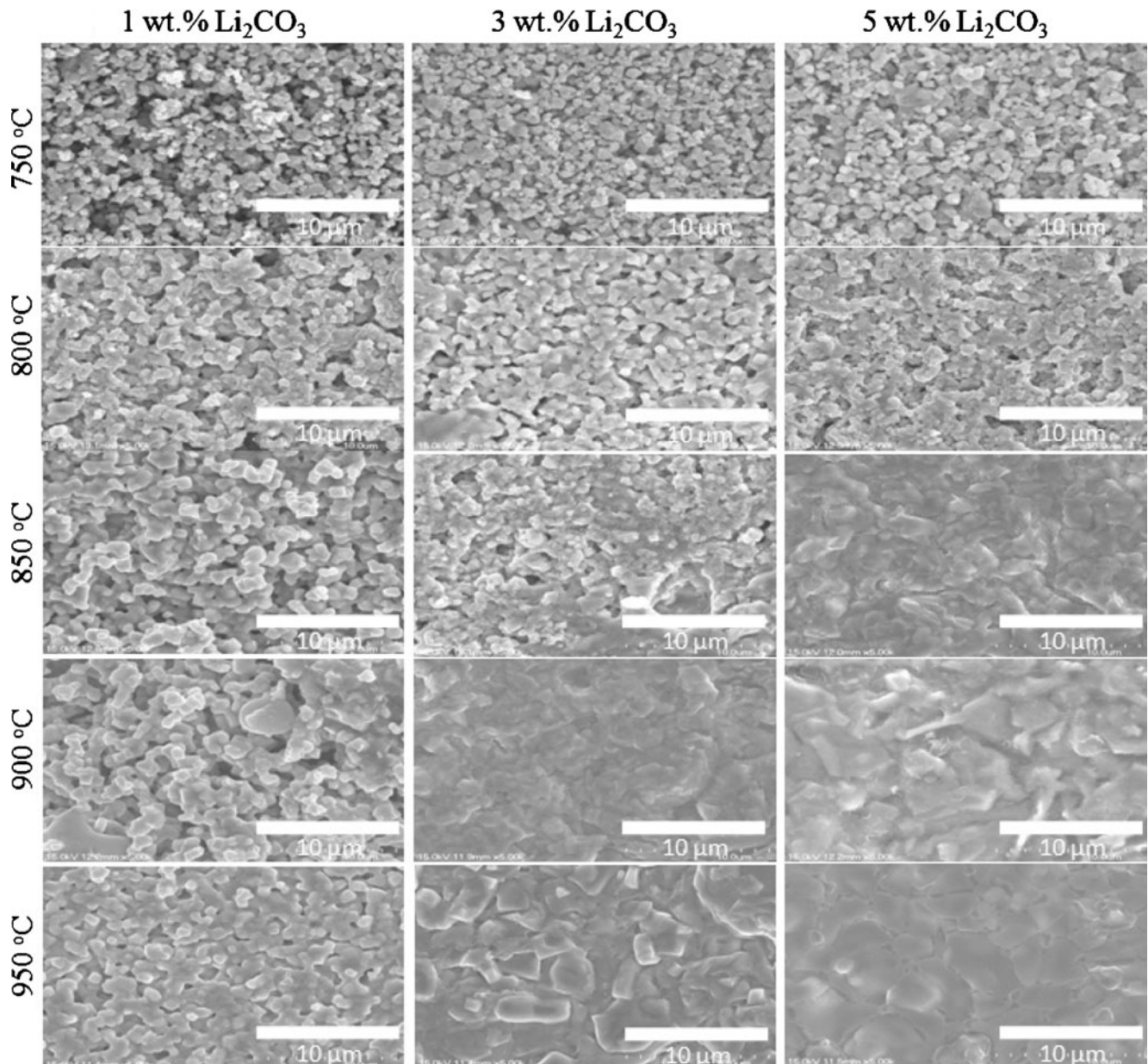


**Fig. 4** The microstructure of 1, 3 and 5 wt.%  $\text{Li}_2\text{CO}_3$  doped BST ceramics sintered at various temperatures (white basic bar length: 10  $\mu\text{m}$ )

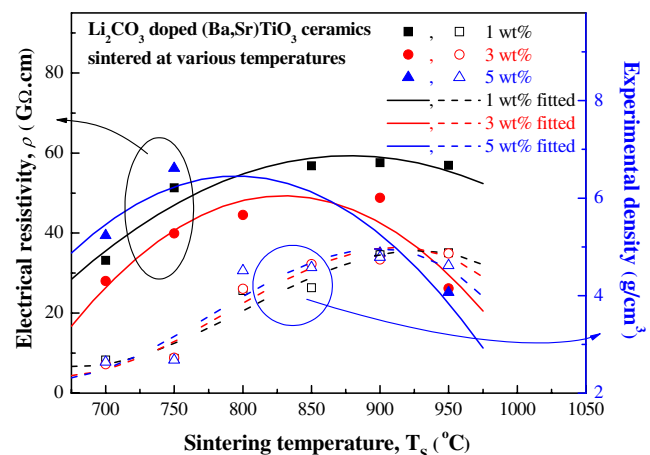
position than others due to the ionic size of  $\text{Li}^+$  is smaller than ionic size of  $\text{Ba}^{2+}$  and  $\text{Sr}^{2+}$  [10, 11]. Therefore, we believe increased bonding energy can be decreased the lattice parameters.

Figure 2 reveals that the frequency dependent relative dielectric permittivity,  $\epsilon_r'$  and dielectric loss of 1, 3, and 5 wt.%  $\text{Li}_2\text{CO}_3$  doped BST ceramics sintered at  $900^\circ\text{C}$ . Frequency dependent relative dielectric permittivity and dielectric loss were respectively investigated from 1 kHz to 100 kHz range. In this range, each sample shows the weak frequency dispersion of relative dielectric permittivity. In case of 1 wt.%  $\text{Li}_2\text{CO}_3$  doped BST ceramic, the relative dielectric permittivity was decreased 0.905% with increasing frequency. As shown in the Fig. 2, the relative dielectric permittivity of 1, 3, and 5 wt.%  $\text{Li}_2\text{CO}_3$  doped BST ceramics was decreased with the increased amount of  $\text{Li}_2\text{CO}_3$ . The relative dielectric permittivity of 1, 3, and 5 wt.%  $\text{Li}_2\text{CO}_3$  doped BST ceramics were 1441, 1194, and 906 at 100 kHz, respectively. Among them, 3 wt.%  $\text{Li}_2\text{CO}_3$  doped BST ceramic shows the smallest value in this experiment. The dielectric loss of 3 wt.%  $\text{Li}_2\text{CO}_3$  doped BST ceramic was 0.0042 at 100 kHz. We found that this low loss tangent probably related with the crystal properties and sintering process. Generally, the cubic structure had the low loss tangent than tetragonal structure [12]. Therefore, we found the decreasing loss tangent was related with pseudo-cubic states. However, the 5 wt.%  $\text{Li}_2\text{CO}_3$  doped BST has the high loss tangent than 3 wt.%  $\text{Li}_2\text{CO}_3$  doped BST. We discussed this behavior in the Fig. 4.

Figure 3 indicates that the electric field ( $E$ ) dependent leakage current density ( $j$ ) of 1, 3, and 5 wt.%  $\text{Li}_2\text{CO}_3$  doped BST ceramics sintered at  $900^\circ\text{C}$  in the electric field of  $\pm 606$  V/cm range. This leakage current density vs. electric field characteristics measured from the maximum reverse bias, through zero to the maximum forward bias. Ten seconds delay time was employed to reduce the relaxation current. The leakage current density of  $\text{Li}_2\text{CO}_3$  doped BST ceramics was increased with the amount of dopants. The leakage current density of 1, 3, and 5 wt.%  $\text{Li}_2\text{CO}_3$  doped BST ceramics was 0.153, 0.369 and  $0.755$  nA/cm<sup>2</sup> at electric field of 606 V/cm, respectively. In general, the electrical resistivity of dielectric materials was increased as the density of the dielectric materials was increased. The density of  $\text{Li}_2\text{CO}_3$  doped BST ceramics was increased with the increased amount of  $\text{Li}_2\text{CO}_3$  in our experiments. However, increased  $\text{Li}_2\text{CO}_3$  dopant has influence on ionic conduction properties in the leakage current mechanism [9]. In spite of increasing density, the whole dielectric performances of  $\text{Li}_2\text{CO}_3$  doped BST ceramics such as relative dielectric permittivity, dielectric loss and electrical properties were degenerated by increasing the amount of  $\text{Li}_2\text{CO}_3$ .

Figure 4 shows the microstructure of 1, 3, and 5 wt.%  $\text{Li}_2\text{CO}_3$  doped BST ceramics sintered at various temperatures. As shown in the Fig. 4, the grain size of  $\text{Li}_2\text{CO}_3$  doped BST ceramics was increased with the elevated sintering temperature. Also, the amount of  $\text{Li}_2\text{CO}_3$  was increased, the density of  $\text{Li}_2\text{CO}_3$  doped BST ceramics was increased at the same temperatures. Until  $800^\circ\text{C}$ , we found the porous ceramics and grains did not revealed necked structure altogether. As increasing the sintering temperature above  $800^\circ\text{C}$ , grain in the  $\text{Li}_2\text{CO}_3$  doped BST ceramic was necked with neighboring grains and then the grain size was increased rapidly. Over the  $800^\circ\text{C}$ , necking process of grains happened and grain size was increased with increasing sintering temperature. By introducing the  $\text{Li}_2\text{CO}_3$  dopant, the sintering temperature was decreased except for the 5 wt.%  $\text{Li}_2\text{CO}_3$  doped BST ceramic. We found that 5 wt.%  $\text{Li}_2\text{CO}_3$  doped BST ceramic were over sintered states at  $900^\circ\text{C}$ .

Figure 5 displays the electrical resistivity and experimental density of 1, 3, and 5 wt.%  $\text{Li}_2\text{CO}_3$  doped BST ceramics sintered at various temperatures. By considering the FE-SEM images and densities of  $\text{Li}_2\text{CO}_3$  doped BST ceramics, sintered at  $900^\circ\text{C}$ , we found that the grains became closed packed (Fig. 4) and the density was increased (Fig. 5). In our experiment, the electrical resistivity of 1, 3 and 5 wt.%  $\text{Li}_2\text{CO}_3$  doped BST ceramics sintered at  $700^\circ\text{C}$  was 33.2, 28.0 and  $39.4$  G $\Omega$ ·cm, respectively. Also, the electrical resistivity of 1, 3 and 5 wt.%  $\text{Li}_2\text{CO}_3$  doped BST ceramics sintered at  $750^\circ\text{C}$  was 51.3, 39.9 and  $56.2$  G $\Omega$ ·cm, respectively. However, the electrical resistivity of 1, 3 and 5 wt.%  $\text{Li}_2\text{CO}_3$  doped BST ceramics sintered at  $900^\circ\text{C}$  was 57.6, 48.8 and  $35$  G $\Omega$ ·cm, respectively. As shown in the Fig. 5, the electrical resistivity and experimental density had the maximum value near the  $850\sim 900^\circ\text{C}$ , and the electrical resistivity and experimental density decreased with increasing



**Fig. 5** The variation of electrical resistivity and experimental density of 1, 3 and 5 wt.%  $\text{Li}_2\text{CO}_3$  doped BST ceramics. Each sample was sintered at various temperatures from  $700^\circ\text{C}$  to  $950^\circ\text{C}$ , respectively

sintering temperature. Especially, the 5 wt.% doped BST ceramics become over sintered phase above 900°C. Therefore experimental density and resistivity of 5 wt.% doped BST ceramics were degenerated.

#### 4 Conclusions

We fabricated the 1, 3, and 5 wt.%  $\text{Li}_2\text{CO}_3$  doped BST ceramics sintered at various temperatures. From this experiment, we found that the  $\text{Li}_2\text{CO}_3$  doped BST ceramics were completely sintered at 900°C. However, we found the pyrochlore phase in the X-ray diffraction pattern of 5 wt.%  $\text{Li}_2\text{CO}_3$  doped BST ceramic. We found that this unexpected pyrochlore phase was related with the over sintered phase of 5 wt.%  $\text{Li}_2\text{CO}_3$  doped BST ceramic.

By introducing the  $\text{Li}_2\text{CO}_3$  dopant to the BST system, the lattice parameters were decreased due to the increased strong chemical bonding energy and increased density. Cubic structure of pure BST, 1 wt%  $\text{Li}_2\text{CO}_3$  doped BST, and 3 wt %  $\text{Li}_2\text{CO}_3$  doped BST has the low loss tangent than that of 5 wt%  $\text{Li}_2\text{CO}_3$  doped BST. This behavior come from the pyrochlore phase, originated from the over sintering property.

**Acknowledgement** This work was financially supported by the Fundamental R&D Program for Core Technology of Materials funded

by the Ministry of Knowledge Economy, Republic of Korea and Basic Science Research Program through the National Research Foundation of Korea (NRF) funded by the Ministry of Education, Science and Technology (grant number 2010-0011536).

#### References

1. S.-G. Lee, S.E. Moon, H.-C. Ryu, M.-H. Kwak, Y.-T. Kim, *Appl. Phys. Lett.* **82**, 2133 (2003)
2. K.-T. Kang, I.D. Kim, M.-H. Lim, H.-G. Kim, J.-M. Hong, *Thin. Solid. Films.* **516**, 1218 (2008)
3. J.B. Lim, J. Son, S. Nahm, W. Lee, M. Yoo, N.G. Gang, H.J. Lee, Y.S. Kim, *Jpn. J. Appl. Phys.* **43**, 5388 (2004)
4. T. Hu, H. Jantunen, A. Uusimaki, S. Leppavuori, *Materials Science in Semiconductor Processing* **5**, 215 (2003)
5. X.L. Li, H.A. Ma, Y.J. Zheng, Y. Liu, G.H. Zuo, W.Q. Liu, J.G. Li, X. Jia, *J. Alloys and Compounds* **463**, 412 (2008)
6. T. Tick, J. Perantie, H. Jantunen, A. Uusimaki, *J. Eur. Ceram. Soc.* **28**, 839 (2008)
7. J.B. Lim, J. Son, S. Nahm, W. Lee, M. Yoo, N.G. Gang, H.J. Lee, Y.S. Kim, *Jpn. J. Appl. Phys.* **43**, 5388 (2004)
8. C.L. Huang, R.J. Lin, J.-J. Wang, *Jpn. J. Appl. Phys.* **41**, 758 (2002)
9. H.-W. You, J.-H. Koh, *Jpn. J. Appl. Phys.* **45**, 6362 (2006)
10. S.Y. Jeon, I.S. Kim, B.K. Min, J.S. Song, J.D. Yoon, *Journal of the Korean Ceramic Society* **43**, 421 (2006)
11. X. Wang, W. Lu, J. Liu, Y. Zhou, D. Zhou, *J. Eur. Ceram. Soc.* **26**, 1981 (2006)
12. G. A. Smolenskii, *Ferroelectrics and related materials* (Amsterdam, Netherlands, 1984).